Monthly Notices of the ROYAL ASTRONOMICAL SOCIETY

MNRAS **533,** 63–66 (2024) https://doi.org/10.1093/mnras/stae1765
Advance Access publication 2024 August 7

Correction to: Conversions between gas-phase metallicities in MaNGA

by Jillian M. Scudder [1]★ Sara L. Ellison [2] Loubna El Meddah El Idrissi[1] and Henry Poetrodjojo [3,4]

[1]*Department of Physics & Astronomy, Oberlin College, Oberlin, OH 44074, USA*
[2]*Department of Physics & Astronomy, University of Victoria, Finnerty Road, Victoria, BC V8P 1A1, Canada*
[3]*Research School of Astronomy and Astrophysics, The Australian National University, Cotter Road, Weston, ACT 2611, Australia*
[4]*ARC Centre of Excellence for All Sky Astrophysics in 3 Dimensions (ASTRO 3D), Australia*

Key words: errata, addenda – galaxies: abundances – galaxies: statistics – galaxies: general – galaxies: ISM.

We have identified an error in the calculation of O3N2-based calibrations presented in Scudder et al. (2021), which were metallicities based on Pettini & Pagel (2004) O3N2, Marino et al. (2013) O3N2, and Curti et al. (2017) O3N2. [O III] fluxes were mistakenly multiplied by 1.33, which is required for R_{23}-based calibrations but not for the ([O III]λ5007/Hβ)/([N II]λ6584/Hα) line ratio. Correcting these values systematically decreases the raw metallicity values for these three calibrations, and slightly increases the number of overall spaxels with metallicities. A corrected Table 1 with metallicity values is presented here. All three metallicity catalogues (DR15, DR7, and TYPHOON) were identically processed, and have all now been corrected. We have re-run the rest of the work, and find that the scatter around our polynomial fits is functionally unaffected. We have updated table 3 of Scudder et al. (2021) here as Table 2 for completeness.

The polynomial fits themselves shift horizontally or vertically when converting from or to an O3N2-based metallicity calibration into a non-O3N2-based calibration, by somewhere between 0.026 and 0.055 dex. The median magnitude of the vertical shifts between polynomials is 0.032 dex. Conversions between O3N2-based calibrations and other O3N2-based calibrations are unaffected. We show a sample figure in Fig. 1. We have updated the polynomials presented in Appendix Table A1, and in the full tables presented in the supplementary material.

Fig. 7 of Scudder et al. (2021) is the most directly impacted figure; qualitatively it is virtually the same, as all three populations presented in that figure were affected by the same systematic error, and for completeness we reproduce it here in Fig. 2. The right hand panel of fig. 8 of Scudder et al. (2021) is the only figure that has a visible change with the update of these metallicities, with the reduction of offsets between polynomials for PP04 O3N2-based metallicities into any other metallicities reduced by 0.04 dex to 0.1 dex. We thus show it here as Fig. 3. The median offset across all polynomials is only reduced by 0.003 dex relative to that reported in Scudder et al. (2021).

All remaining figures in Scudder et al. (2021) are affected by $\lesssim$ 0.003 dex, with the updated typically reducing scatter, and are not visibly different from those published. Values in text are either identical or correct within 0.003 dex. Tables not reproduced here are also completely unchanged from the original published version. Supplementary online materials (all versions of figs 2, 3, 4, 7 in Scudder et al. 2021, and the full tables of polynomials) have been fully updated.

Table 1. Total number of metallicity values per calibration, for both the SMC and MW dust correction models, after S/N cuts, BPT classifications, and including an Hα EW cut.

Calibration	SMC spaxels	MW spaxels
Z94	1047 232	858 244
M91	1060 728	953 147
KK04	1065 094	989 498
KE08	1069 318	1027 191
D16	1012 424	890 787
PP04 N2	1091 383	1055 164
M13 N2	1092 348	1055 271
C17 N2	1081 521	1051 017
PP04 O3N2	1091 786	1054 508
M13 O3N2	1087 266	1048 824
C17 O3N2	1092 355	1055 359

Note. All abbreviations are defined as in Scudder et al. (2021).

★ E-mail: jillian.scudder@oberlin.edu

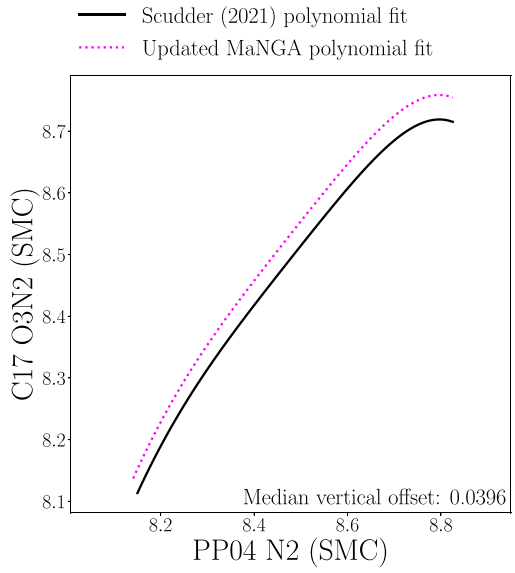

Figure 1. Comparison of a polynomial lines of best fit as published in Scudder et al. (2021) in a solid black line, and the corrected metallicities in a pink dotted line. The median vertical offset between polynomials for the range in x values with polynomial coverage is plotted in the lower left corner. In this case, the difference between polynomials is about 0.04 dex. This figure is representative of the change in the polynomials.

Table 2. In ascending typical 2σ scatter, we present the emission-line permutations between calibrations. For each set of calibrations which match the inclusions/exclusions, we find the typical offset of the 2σ contour (the median absolute value of the 2σ residuals) from our polynomial fit. We also include the smallest and largest 2σ residuals for each set. The median (and range) of the 2σ scatter is smallest for all calibrations which have full overlap in their emission-line requirements: the top row includes all of the O3N2-based calibrations.

Lines excluded (x but not y)	Lines in overlap (x and y)	2σ scatter (dex)		
		$\mu_{1/2}$	min	max
Full overlap	[O III], H α, [N II], H β	0.0025	0.0022	0.0036
Full overlap	H α, [N II]	0.0525	0.002	0.1549
Full overlap	[O II], [O III], [N II], H β	0.0602	0.0135	0.1412
H β, [O III]	H α, [N II]	0.0613	0.0477	0.0919
H β, [S II]	H α, [N II]	0.0697	0.0522	0.0895
[S II]	H α, H β, [N II]	0.0792	0.0712	0.1127
[O II]	H β, [N II], [O III]	0.0897	0.0615	0.1391
H β, [O II], [O III]	[N II]	0.1124	0.0674	0.1767
H α	H β, [N II], [O III]	0.144	0.108	0.1599
H α, [S II]	H β, [N II]	0.1564	0.1358	0.1863
H α	[N II]	0.1724	0.117	0.2023
[O III]	H α, H β, [N II]	0.1907	0.1892	0.1997
[O II], [O III]	H β, [N II]	0.2687	0.1802	0.2838

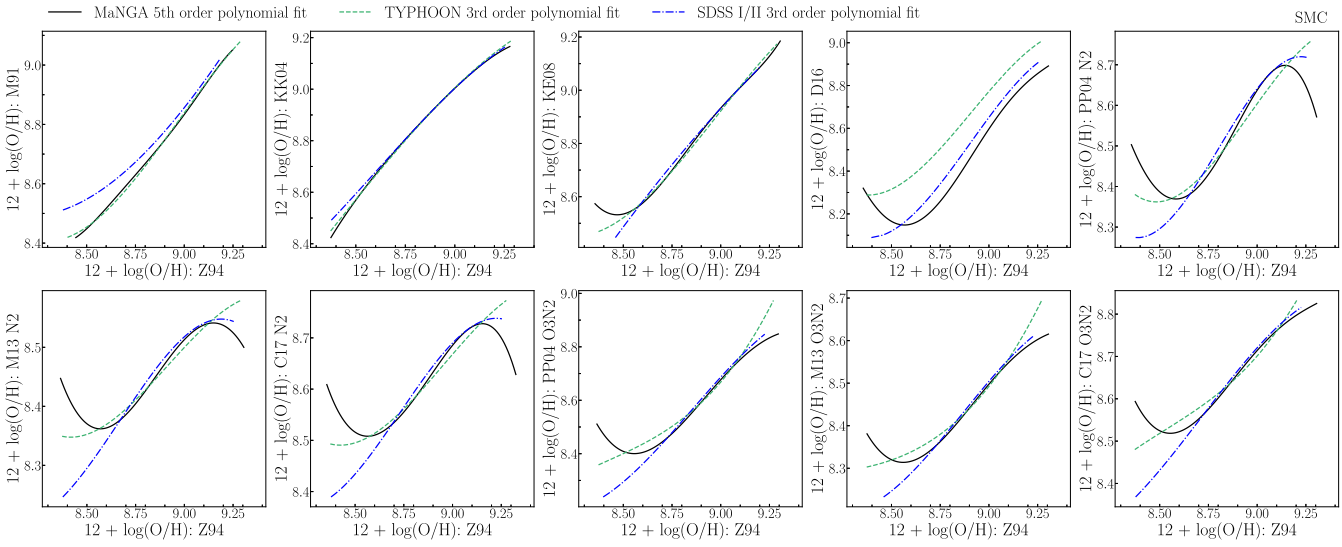

Figure 2. Comparison of the polynomial lines of best fit. The fifth-order polynomial fit to the MaNGA data presented here are plotted in a black solid line. We plot the third-order polynomial fits to the DR7, which are also affected by this metallicity erratum, in a blue dot-dashed line. third-order polynomial fits to the TYPHOON data, also recalculated here, are plotted in a dashed green line.

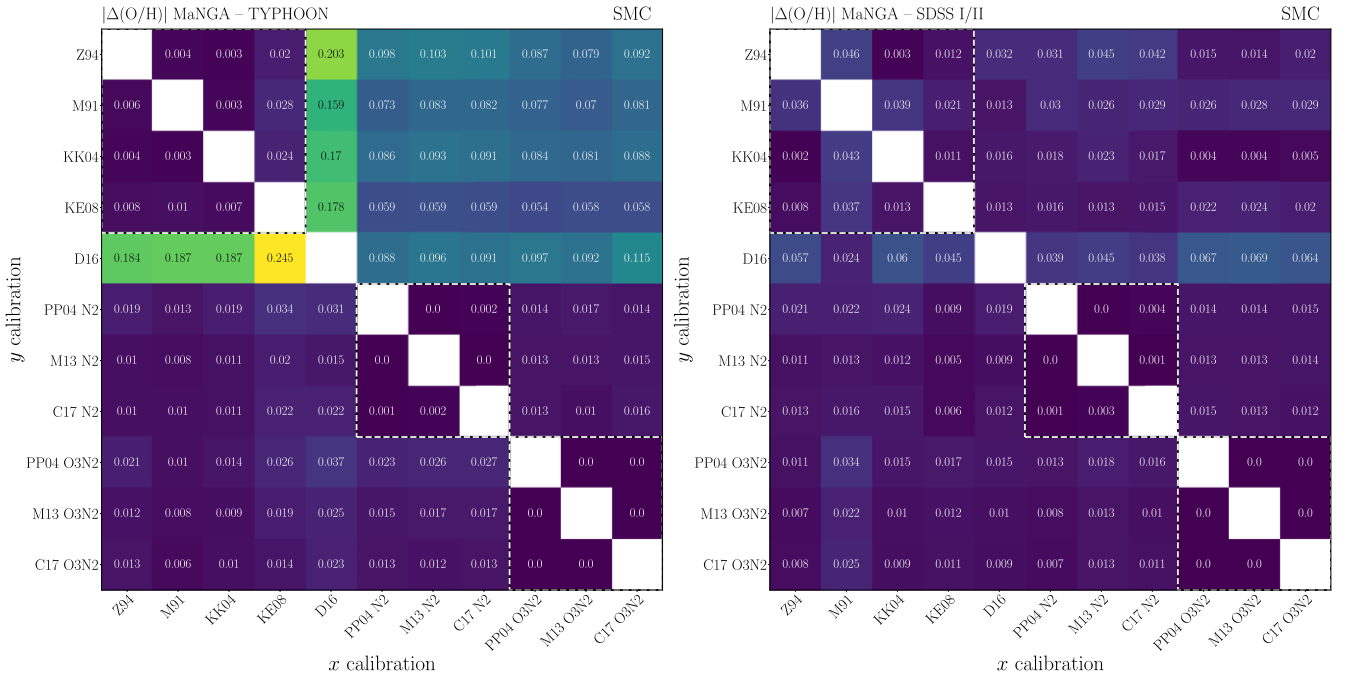

Figure 3. Comparison of the differences between polynomial lines of best fit. The left panel is functionally unchanged, with median offsets still at 0.019 dex. The median difference between MaNGA & DR7 (right) is reduced by 0.003 dex to 0.014 dex, with the published trend of PP04 O3N2 metallicities being slightly more offset now removed.

DATA AVAILABILITY

The emission-line data underlying Scudder et al. (2021) are publicly available as part of the MaNGA DR17 data release, available at https://www.sdss.org/dr17/. Metallicity values themselves are available upon reasonable request to the corresponding author.

REFERENCES

Curti M., Cresci G., Mannucci F., Marconi A., Maiolino R., Esposito S., 2017, MNRAS, 465, 1384
Marino R. A. et al., 2013, A&A, 559, A114
Pettini M., Pagel B. E. J., 2004, MNRAS, 348, L59
Scudder J. M., Ellison S. L., El Meddah El Idrissi L., Poetrodjojo H., 2021, MNRAS, 507, 2468

SUPPORTING INFORMATION

Supplementary data are available at *MNRAS* online.

Supplementary Materials.zip

Please note: Oxford University Press is not responsible for the content or functionality of any supporting materials supplied by the authors. Any queries (other than missing material) should be directed to the corresponding author for the article.

APPENDIX A: TABLES

In this Appendix, we provide a sample few rows of the tables which list conversions between all calibrations, the number of spaxels used in the fitting procedure, the range of validity, and the polynomial fits used in this work as an example of the data structure.

Table A1. Summary of the median offset from a fifth-order polynomial best fit in both positive and negative directions, for the contour that encloses 95.5 per cent of the data. For each metallicity calibration pairing, the number of spaxels which are present is also recorded, for the SMC dust correction curve. The full table, along with the same for all other pairings, and for the MW dust correction curve, is available as supplementary material.

Conversion $x \rightarrow y$	n spaxels	2σ scatter	Range of validity $(12 + \log(\mathrm{O/H}))$	Polynomial fit: $a + bx + cx^2 + dx^3 + ex^4 + fx^5$				
				a	b	c	d	e	f
Z94 → PP04 O3N2	1047174	[−0.1235, 0.1251]	[8.3647, 9.2955]	−8255.57111302	+5500.47948047	−1412.33588325	+176.61349745	−10.82276874	+0.26107276
Z94 → M13 O3N2	1046104	[−0.0826, 0.0836]	[8.3745, 9.3053]	−21025.73022481	+12464.89658234	−2935.1585598	+343.53656396	−19.99737841	+0.46338882
Z94 → C17 O3N2	1047150	[−0.0891, 0.085]	[8.3745, 9.3051]	−30018.98525082	+17956.62194749	−4268.0189955	+504.38192063	−29.65474639	+0.69430492
M91 → Z94	1037616	[−0.0264, 0.0206]	[8.4035, 9.0696]	−82822.51326969	+51125.46960079	−12549.66580389	+1532.47593546	−93.14893094	+2.25576348
M91 → KK04	1055420	[−0.0199, 0.0098]	[8.4035, 9.0712]	+49862.66651585	−26473.36992983	+5590.08956813	−586.27362519	+30.50799985	−0.62930761
		lower branch:	[7.8508, 8.2351]	−25.16773802	+7.44906684	−0.40975953			
...	...	...	...	...	...	...	...	...	...

This paper has been typeset from a TEX/LATEX file prepared by the author.